

# Electrical transport along bacterial nanowires from *Shewanella oneidensis* MR-1

Mohamed Y. El-Naggar<sup>a,1</sup>, Greg Wanger<sup>b</sup>, Kar Man Leung<sup>c,d</sup>, Thomas D. Yuzvinsky<sup>a</sup>, Gordon Southam<sup>e</sup>, Jun Yang<sup>c</sup>, Woon Ming Lau<sup>d</sup>, Kenneth H. Nealson<sup>b,f</sup>, and Yuri A. Gorby<sup>b</sup>

<sup>a</sup>Department of Physics and Astronomy, <sup>f</sup>Departments of Earth Sciences and Biological Sciences, University of Southern California, Los Angeles, CA 90089; <sup>b</sup>The J. Craig Venter Institute, San Diego, CA 92121; <sup>c</sup>Department of Mechanical and Materials Engineering, University of Western Ontario, London, ON, Canada N6A 5B9; <sup>d</sup>Surface Science Western, University of Western Ontario, London, ON, Canada N6G 0J3; and <sup>e</sup>Department of Earth Sciences, University of Western Ontario, London, ON, Canada N6A 3K7

Edited by James M. Tiedje, Center for Microbial Ecology, East Lansing, MI, and approved August 31, 2010 (received for review April 9, 2010)

**Bacterial nanowires are extracellular appendages that have been suggested as pathways for electron transport in phylogenetically diverse microorganisms, including dissimilatory metal-reducing bacteria and photosynthetic cyanobacteria. However, there has been no evidence presented to demonstrate electron transport along the length of bacterial nanowires. Here we report electron transport measurements along individually addressed bacterial nanowires derived from electron-acceptor-limited cultures of the dissimilatory metal-reducing bacterium *Shewanella oneidensis* MR-1. Transport along the bacterial nanowires was independently evaluated by two techniques: (i) nanofabricated electrodes patterned on top of individual nanowires, and (ii) conducting probe atomic force microscopy at various points along a single nanowire bridging a metallic electrode and the conductive atomic force microscopy tip. The *S. oneidensis* MR-1 nanowires were found to be electrically conductive along micrometer-length scales with electron transport rates up to  $10^9$ /s at 100 mV of applied bias and a measured resistivity on the order of 1  $\Omega$ -cm. Mutants deficient in genes for c-type decaheme cytochromes MtrC and OmcA produce appendages that are morphologically consistent with bacterial nanowires, but were found to be nonconductive. The measurements reported here allow for bacterial nanowires to serve as a viable microbial strategy for extracellular electron transport.**

bioelectronics | microbial fuel cells | bioenergy

Electron transfer is fundamental to biology: organisms extract electrons from a wide array of electron sources (fuels) and transfer them to electron acceptors (oxidants). Prokaryotes can use a wide variety of dissolved electron acceptors (such as oxygen, nitrate, and sulfate) that are accessible to their intracellular enzymes. However, dissimilatory metal-reducing bacteria (DMRB) are challenged by the low solubility of solid phase Fe(III) and Mn(IV) minerals that serve as their terminal electron acceptors, and therefore use extracellular electron transfer to overcome this obstacle (1). Various strategies of extracellular electron transfer have been reported for metal-reducing bacteria, including naturally-occurring (2) and biogenic (3–5) soluble mediators that shuttle electrons from cells to acceptors, as well as direct transfer using multiheme cytochromes associated with the outer membrane (6). Recent reports have also suggested that extracellular electron transport may be facilitated by conductive filamentous extracellular appendages called bacterial nanowires (7–9). The first report found bacterial nanowires in the DMRB *Geobacter* (7). A subsequent scanning tunneling microscopy study (8) demonstrated transverse electrical conduction in nanowires from other microorganisms, including another metal reducer (*Shewanella oneidensis* MR-1), an oxygenic photosynthetic cyanobacterium (*Synechocystis* PCC6803), and a thermophilic fermentative bacterium (*Pelotomaculum thermopropionicum*), when cultivated under conditions of electron acceptor limitation.

To date, several biological assays have demonstrated results consistent with electron transport along bacterial nanowires,

including measurements of improved electricity generation in microbial fuel cells and enhanced microbial reduction of solid-phase iron oxides (7, 8, 10). However, our direct knowledge of nanowire conductivity has been limited to local measurements of transport only across the thickness of the nanowires (7–9). Thus far, there has been no evidence presented to verify electron transport along the length of bacterial nanowires, which can extend many microns, well beyond a typical cell's length. Here we report electron transport measurements along individually addressed bacterial nanowires derived from electron-acceptor limited cultures of the DMRB *S. oneidensis* MR-1.

## Results

**Direct Transport Measurements Using Nanofabricated Electrodes.** To fabricate two-contact devices, chemically fixed samples from continuous cultures were deposited on SiO<sub>2</sub>/Si substrates with prepatterned metallic contact pads. The substrates were subsequently dehydrated in ethanol, critical-point dried, and examined using a dual-column scanning electron/focused ion beam (FIB) microscope. Individual bacterial nanowires were located using secondary electron imaging and were then contacted by ion beam- or electron beam-induced deposition of platinum electrodes (Fig. 1). Current-voltage (I-V) sweeps were collected at ambient conditions using probe stations instrumented to semiconductor parameter analyzers.

Fig. 2 illustrates the results from a single bacterial nanowire extending from a wild-type *S. oneidensis* MR-1 cell. Following deposition of the Pt contacts (Fig. 2A), we observed an ohmic current response to applied voltage (Fig. 2C) with resistance  $R = 386$  M $\Omega$ , yielding a corresponding electron transport rate, at 100 mV, of about  $10^9$  electrons per second. The resistivity estimated from this measurement is 1  $\Omega$ -cm (*Materials and Methods*), comparable in magnitude to that of moderately doped silicon nanowires (11). To confirm that the nanowire provides the only conductive path between the electrodes, a FIB was used to cut the nanowire without disturbing the rest of the device (Fig. 2B). After the nanowire was cut, there was no measurable current response to applied voltage (Fig. 2C), confirming that the observed conduction path was indeed through the nanowire. In addition to the nanowire of Fig. 2, two more bacterial nanowires, sampled from a different bioreactor, were investigated for electrical transport using nanofabricated electrodes, resulting in

Author contributions: M.Y.E.-N., K.M.L., G.S., J.Y., W.M.L., K.H.N., and Y.A.G. designed research; M.Y.E.-N., G.W., K.M.L., T.D.Y., and Y.A.G. performed research; M.Y.E.-N., G.W., K.M.L., T.D.Y., J.Y., W.M.L., K.H.N., and Y.A.G. analyzed data; and M.Y.E.-N., K.M.L., T.D.Y., and Y.A.G. wrote the paper.

The authors declare no conflict of interest.

This article is a PNAS Direct Submission.

<sup>1</sup>To whom correspondence should be addressed. E-mail: mnaggar@usc.edu.

This article contains supporting information online at [www.pnas.org/lookup/suppl/doi:10.1073/pnas.1004880107/-DCSupplemental](http://www.pnas.org/lookup/suppl/doi:10.1073/pnas.1004880107/-DCSupplemental).

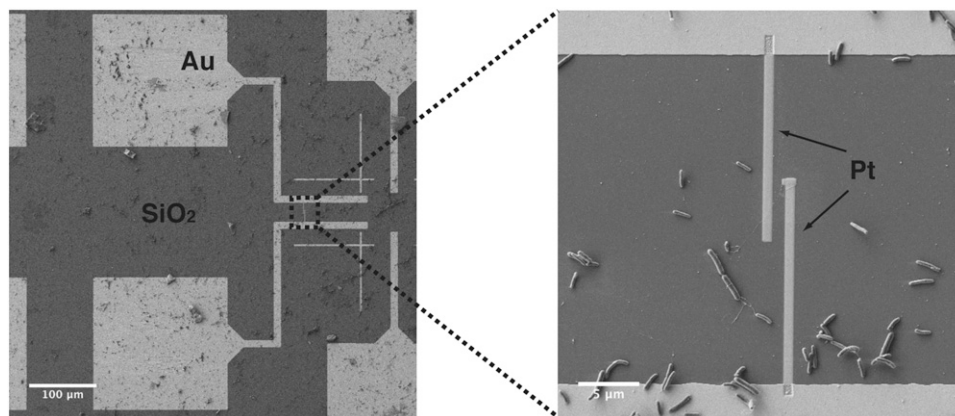


**Fig. 1.** Contacting individual bacterial nanowires with nanofabricated Pt electrodes. SEM images showing the geometry of the prefabricated Au contacts on SiO<sub>2</sub>/Si. The zoom-in shows the FIB-deposited Pt contacts addressing a bacterial nanowire emanating from a *S. oneidensis* MR-1 cell.

measured resistivities of 4 Ω-cm ( $R = 465 \text{ M}\Omega$ ) (Fig. S14) and 17 Ω-cm ( $R = 2.3 \text{ G}\Omega$ ) (Fig. S1B).

**Conducting Probe Atomic Force Microscopy.** To determine whether the resistivity values obtained from our two-contact devices include a significant contribution from contact resistance between electrodes and nanowires, conducting probe atomic force microscopy (CP-AFM) was used to measure the resistance of a single nanowire as a function of its length. CP-AFM is a convenient tool for probing local electrical properties at the nanometer scale, and has been increasingly used for the electrical characterization of biological molecules (12–14). CP-AFM was also previously employed to demonstrate transverse conduction through bacterial nanowires produced by *Geobacter sulfurreducens* (7) and *S. oneidensis* MR-1 (9). In the previous experiments, however, the nanowires were supported on conductive surfaces of highly ordered pyrolytic graphite, precluding measurements of their longitudinal conduction. To verify longitudinal transport along bacterial nanowires using CP-AFM, *S. oneidensis* MR-1 nanowires from chemically fixed samples were immobilized on SiO<sub>2</sub>/Si substrates with lithographically patterned Au microgrids as electrodes (Fig. 3A).

Electronic transport along a nanowire in contact with the Au microgrid was measured by using the Pt-coated AFM tip as

a second electrode. With the AFM tip at the position shown in Fig. 3B, ~600 nm away from the Au electrode and in contact with the nanowire, we obtained the I-V curve shown in Fig. 3C. The current response to the applied voltage was found to be approximately linear and consistent with the results obtained using nanofabricated Pt electrodes (Fig. 2). As a control, we observed that whenever the AFM tip was placed directly on the SiO<sub>2</sub> surface, we obtained a background current of ~10 pA (Fig. 3C, Inset), confirming that extraneous conduction through adsorbed water layers or other contaminants was negligible.

Fig. 3D shows multiple measurements on the same nanowire at different points along its length. We observed a linear relationship between measured resistance and length, allowing us to extrapolate the curve to zero length to estimate the overall contact resistance. We obtained a value of 58 MΩ that, when subtracted from the total resistance, yields a bulk resistivity for the nanowire on the order of 1 Ω-cm, in agreement with measurements using nanofabricated Pt electrodes (Fig. 2).

**Nonconductive Appendages Produced by *S. oneidensis* MR-1 Mutants Deficient in MtrC and OmcA.** We also studied mutants ( $\Delta\text{mtrC}/\text{omcA}$ ) lacking genes for multiheme *c*-type cytochromes MtrC and OmcA (8). The  $\Delta\text{mtrC}/\text{omcA}$  mutants were cultivated in continuous flow bioreactors under identical conditions as wild-

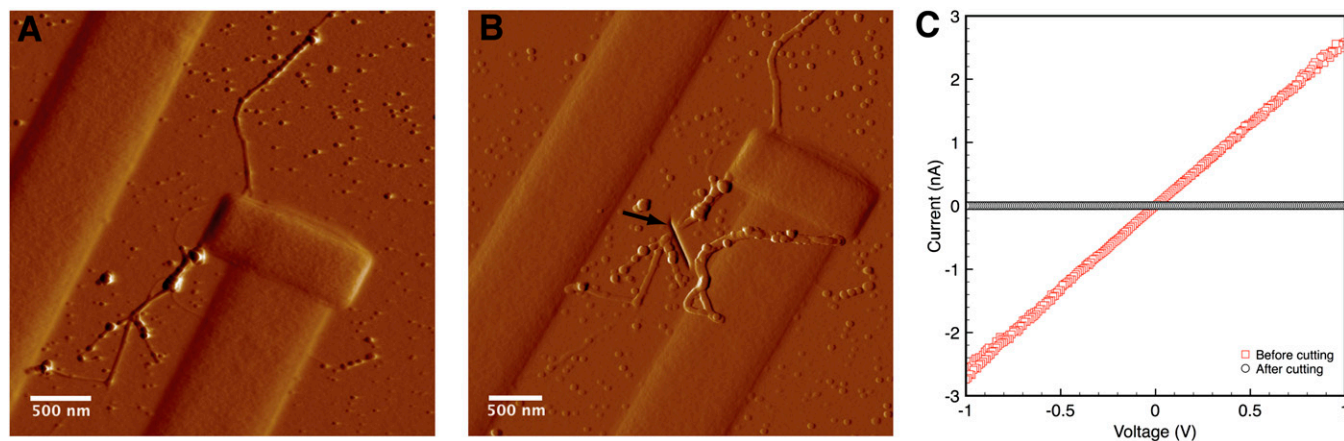


**Fig. 2.** Measuring electrical transport along a bacterial nanowire. (A) Tapping-mode atomic force microscopy (AFM) amplitude image detailing the contact area with the bacterial nanowire from Fig. 1. (B) Contact-mode AFM deflection image of the junction after cutting the nanowire with FIB milling. The arrow marks the cut location. (C) Current-voltage curve of the bacterial nanowire (ramp-up and ramp-down) both before (red) and after (black) cutting the nanowire.



In conclusion, our data demonstrate electrical transport along bacterial nanowires from *S. oneidensis* MR-1, with transport rates that allow for bacterial nanowires to serve as a viable microbial strategy for extracellular electron transport. The measurements reported here motivate further investigations into the molecular composition and physical transport mechanism of bacterial nanowires, both to understand and realize the broad implications for natural microbial systems and biotechnological applications such as microbial fuel cells.

## Materials and Methods

**Cultivation.** *S. oneidensis* strain MR-1 (wild-type) and the double-deletion mutant  $\Delta\text{mntC}/\text{ComcA}$  lacking two decaheme cytochromes were cultured in continuous flow bioreactors (BioFlo 110; New Brunswick Scientific) with a dilution rate of  $0.05\text{ h}^{-1}$  and an operating liquid volume of 1 L. A chemically defined medium was used with lactate as the sole electron donor, and conditions were maintained as previously described by Gorby et al. (8) to achieve electron acceptor limitation. Appendages were produced in response to electron acceptor ( $\text{O}_2$ ) limitation, when the dissolved  $\text{O}_2$  tension was lowered below the detection of the polarographic  $\text{O}_2$  electrode.

An estimate of the specific respiration rate was calculated as follows: Starting with a wild-type *S. oneidensis* MR-1 bioreactor in steady state condition, cell density was determined using a Petroff-Hauser counting chamber to be  $7.72 \times 10^8$  cells/mL. The flow of growth medium to the reactor was then shut off. Shortly thereafter, all the remaining electron donor (lactate) was consumed, triggering a rapid increase in dissolved  $\text{O}_2$  concentration. Next, lactate was added to the reactor to a final concentration of 50 mM, with the oxidation of lactate immediately causing a rapid decrease in dissolved  $\text{O}_2$  concentration. A subsequent rapid increase in dissolved  $\text{O}_2$  concentration indicated that the lactate had been consumed. By measuring the time it took for the 50 mM lactate to be consumed (180 s), extracting 12 electrons per lactate molecule, and knowing the cell density, we calculate the rate of electron transfer per cell to be  $2.6 \times 10^6$  electrons per cell per second.

**Nanofabricated Devices. Sample preparation.** Samples for electrical measurements using nanofabricated electrodes were removed from steady-state bioreactor cultures and immediately fixed using glutaraldehyde (2.5% concentration). Fixed samples were applied to oxidized Si chips with pre-patterned Au contacts (Fig. 1) and subjected to a serial dehydration protocol using increasing concentrations of ethanol (10, 25, 50, 75, and finally 100% vol/vol ethanol). The dehydrated samples were then critical-point dried and desiccated for further nanofabrication processing.

**Electrode fabrication.** Imaging and deposition were carried out using Zeiss 1540 XB FIB/SEM Etching/Deposition Systems. Cells with attached nanowires were located in the proximity of the prefabricated Au contacts. A Pt precursor was then introduced to the chamber using a gas injection system and electrodes were directly deposited to contact the bacterial nanowires using ion beam- (10 pA FIB current) or electron beam-induced chemical vapor deposition. The electrode sections in contact with the prefabricated Au contacts were always deposited by the FIB (which mills as it deposits), thus cleaning the prefabricated patterns of any cellular material that may have accumulated during sample preparation.

**Electrical measurements.** Current-voltage (I-V) measurements were performed at room temperature using probe stations instrumented to either an Agilent 4156C semiconductor parameter analyzer or an Agilent B1500A analyzer. Results for three successful measurements of transport along bacterial nanowires from three different wild-type *S. oneidensis* MR-1 cells and two different samples are shown in Fig. 2 and Fig. S1. For each nanowire tested, resistance was calculated from the ohmic current-voltage (I-V) trace. Knowing the resistance ( $R$ , in  $\Omega$ ), the resistivity ( $\rho$ , in  $\Omega\text{-cm}$ ) was calculated using  $\rho = \frac{RA}{L}$ , where  $L$  is the length of the nanowire segment between the two probes (measured by SEM or AFM imaging) and  $A$  is the cross sectional nanowire area (calculated using AFM height measurements described below).

**Electrode characterization and controls.** The Pt electrodes deposited by beam induced chemical vapor deposition were characterized separately to assess

their contribution to the measured resistance. Fig. S3A shows a FIB-deposited Pt line (30-nm thick,  $1\text{-}\mu\text{m}$  wide,  $27\text{-}\mu\text{m}$  long) connecting the prefabricated Au patterns. From a current of  $93.2\text{ }\mu\text{A}$  at 1V, the resistivity of the FIB-deposited Pt is calculated to be about  $10^{-3}\text{ }\Omega\text{-cm}$ , including some contribution from the contact resistance between the Pt and prefabricated Au. This resistivity value is higher than the resistivity of bulk Pt, which is expected because of the carbon and gallium contamination inherent in the FIB deposition process, but is still a small contribution to the overall resistance of the junctions involving bacterial nanowires ( $>100\text{ M}\Omega$  in Fig. 2 and Fig. S1). In addition to cutting a bacterial nanowire (Fig. 2), another open-circuit control was conducted (Fig. S3B) by placing two Pt probes very close together ( $<150\text{ nm}$  without a bridging nanowire) on a chip that underwent the same glutaraldehyde fixation, dehydration, and critical-drying protocol as the bacterial nanowire junctions. This sample also showed no current response to applied voltage, further ruling out any metallic contamination between the electrodes under the deposition conditions used in this study. **AFM of nanofabricated devices.** Following nanofabrication and electrical measurements, samples were inspected using a Veeco Innova AFM employing either tapping mode (Fig. 2A) or contact mode (Fig. 2B). The typical appendage height was found to be 8–10 nm (Fig. S4). A typical electrode thickness, for the deposition conditions used here, was 30–40 nm. Repeated AFM scanning after electrode deposition and successful I-V measurements but before cutting the nanowire of Fig. 2 displaced some extracellular debris close to the junction area (e.g., placing material near the right electrode in Fig. 2B compared with Fig. 2A), but the junction remained conductive.

**CP-AFM. Sample preparation.** Au microgrids were fabricated on a  $\text{SiO}_2/\text{Si}$  substrate by standard photolithographic patterning followed by electron-beam vapor deposition of 3 nm of Cr (as an adhesion layer) and 20 nm of Au. Samples were harvested from the bioreactor, fixed using 2.5% glutaraldehyde, and applied to the Au microgrid chips. These chips were air-dried (no dehydration or critical point drying) and washed with deionized water to remove salts in the culture medium.

**Conducting probe atomic force measurements.** An Au microgrid (Fig. 3) was electrically connected to the sample stage of an AFM system (Veeco Dimension V) using silver paint. Pt/Cr coated Si AFM probes (BudgetSensors ContE) with a nominal spring constant of 0.2 N/m were used for both tapping and contact mode imaging. The current vs. voltage (I-V) curves of Fig. 3 were measured in point-spectroscopy mode with a typical gain setting of 1 V/nA. The loading force applied for electrical measurements (Fig. 3) was 4 nN, which we found to be the minimum force required to establish a stable short-circuiting contact between the conductive AFM tip and the Au electrode. In many cases, an imaging force of 10 nN or greater began to dislodge and damage the biological structures. Under such conditions, the apex of the conductive AFM tip could be coated with insulating debris. The minimum force (4 nN) was chosen for the electrical measurements to maintain an intimate electrical contact and not to damage the delicate nanowires. The sample voltage was ramped between  $-1$  and 1 V at 0.2 Hz, yielding consistent and repeatable data. The resistance at each position along the nanowire was calculated using the most linear part ( $\pm 0.4\text{ V}$ ) of the I-V curve.

**ACKNOWLEDGMENTS.** We thank C. Zhou's research group and S. Cabrini for experimental help. Nanofabrication was conducted at the Lawrence Berkeley National Laboratory Molecular Foundry, University of California Riverside Center for Nanoscale Science and Engineering, and the Western Nanofabrication Laboratory. This work was supported by the Air Force Office of Scientific Research MURI FA9550-06-1-0292 and YIP FA9550-10-1-0144. Work at the Molecular Foundry was supported by the Office of Basic Energy Sciences of the US Department of Energy under Contract DE-AC02-05CH11231. This research was partially supported through a grant from the Legler-Benbough Foundation (San Diego, CA), internal funding from the J. Craig Venter Institute, and by the Canadian Natural Science and Engineering Research Council, Interdisciplinary Development Initiatives Program, Canada Foundation for Innovation, and Surface Science Western.

- Chang IS, et al. (2006) Electrochemically active bacteria (EAB) and mediator-less microbial fuel cells. *J Microbiol Biotechnol* 16:163–177.
- Lovley DR, Coates JD, Blunt-Harris EL, Phillips EJP, Woodward JC (1996) Humic substances as electron acceptors for microbial respiration. *Nature* 382:445–448.
- Newman DK, Kolter R (2000) A role for excreted quinones in extracellular electron transfer. *Nature* 405:94–97.
- Marsili E, et al. (2008) *Shewanella* secretes flavins that mediate extracellular electron transfer. *Proc Natl Acad Sci USA* 105:3968–3973.

- von Canstein H, Ogawa J, Shimizu S, Lloyd JR (2008) Secretion of flavins by *Shewanella* species and their role in extracellular electron transfer. *Appl Environ Microbiol* 74: 615–623.
- Myers CR, Myers JM (1992) Localization of cytochromes to the outer membrane of anaerobically grown *Shewanella putrefaciens* MR-1. *J Bacteriol* 174: 3429–3438.
- Reguera G, et al. (2005) Extracellular electron transfer via microbial nanowires. *Nature* 435:1098–1101.

8. Gorby YA, et al. (2006) Electrically conductive bacterial nanowires produced by *Shewanella oneidensis* strain MR-1 and other microorganisms. *Proc Natl Acad Sci USA* 103:11358–11363.
9. El-Naggar MY, Gorby YA, Xia W, Nealon KH (2008) The molecular density of states in bacterial nanowires. *Biophys J* 95:L10–L12.
10. Reguera G, et al. (2006) Biofilm and nanowire production leads to increased current in *Geobacter sulfurreducens* fuel cells. *Appl Environ Microbiol* 72:7345–7348.
11. Yu JY, Chung SW, Heath JR (2000) Silicon nanowires: Preparation, device fabrication, and transport properties. *J Phys Chem B* 104:11864–11870.
12. Cohen H, Nagues C, Naaman R, Porath D (2005) Direct measurement of electrical transport through single DNA molecules of complex sequence. *Proc Natl Acad Sci USA* 102:11589–11593.
13. Andolfi L, Cannistraro S (2005) Conductive atomic force microscopy study of plastocyanin molecules adsorbed on gold electrode. *Surf Sci* 598:68–77.
14. Cai LT, Tabata H, Kawai T (2001) Probing electrical properties of oriented DNA by conducting atomic force microscopy. *Nanotechnology* 12:211–216.
15. McLean JS, et al. (2010) Quantification of electron transfer rates to a solid phase electron acceptor through the stages of biofilm formation from single cells to multicellular communities. *Environ Sci Technol* 44:2721–2727.

# Supporting Information

El-Naggar et al. 10.1073/pnas.1004880107

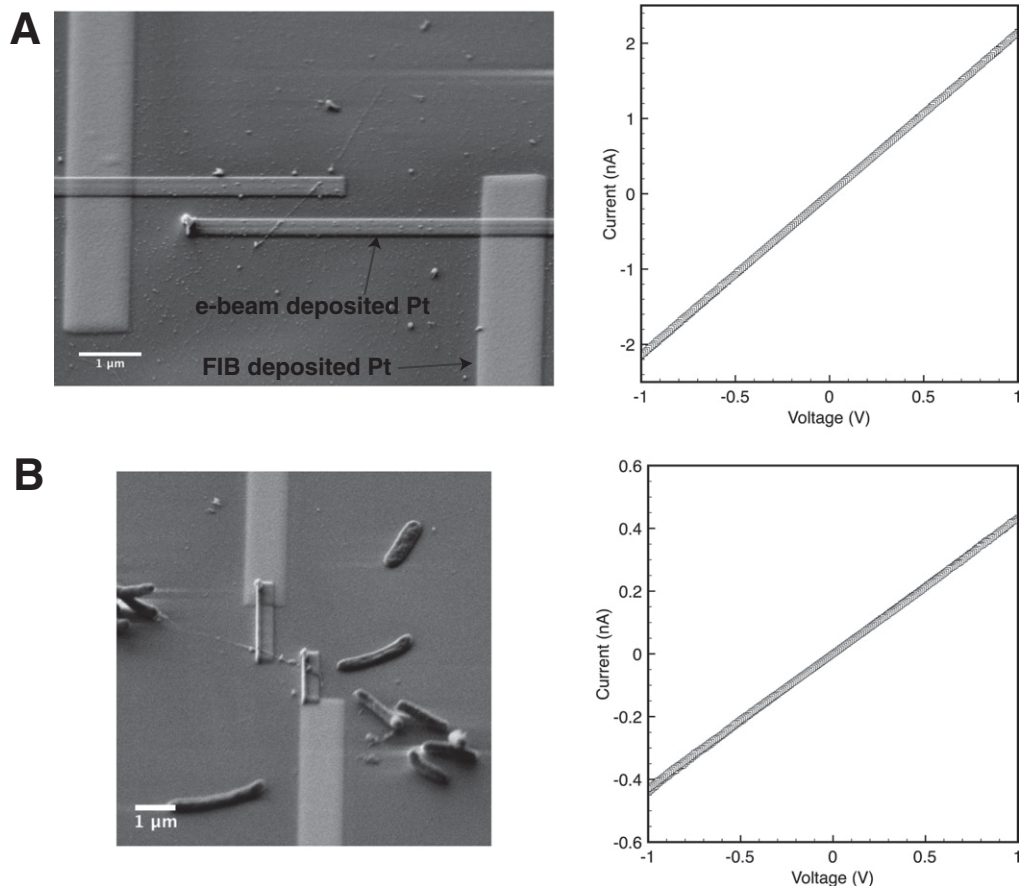


**Fig. S1.** Additional measurements of bacterial nanowires using nanofabricated electrodes. (A) SEM image of a bacterial nanowire addressed by a combination of focused ion beam (FIB) and e-beam deposited Pt contacts along with the current-voltage curve (ramp-up and down). (B) An additional bacterial nanowire (SEM) probed by a combination of FIB and e-beam deposited Pt electrodes and the associated current-voltage curve. SEM images in A and B are tilted by 54° to be at the coincidence point of the electron and FIBs.

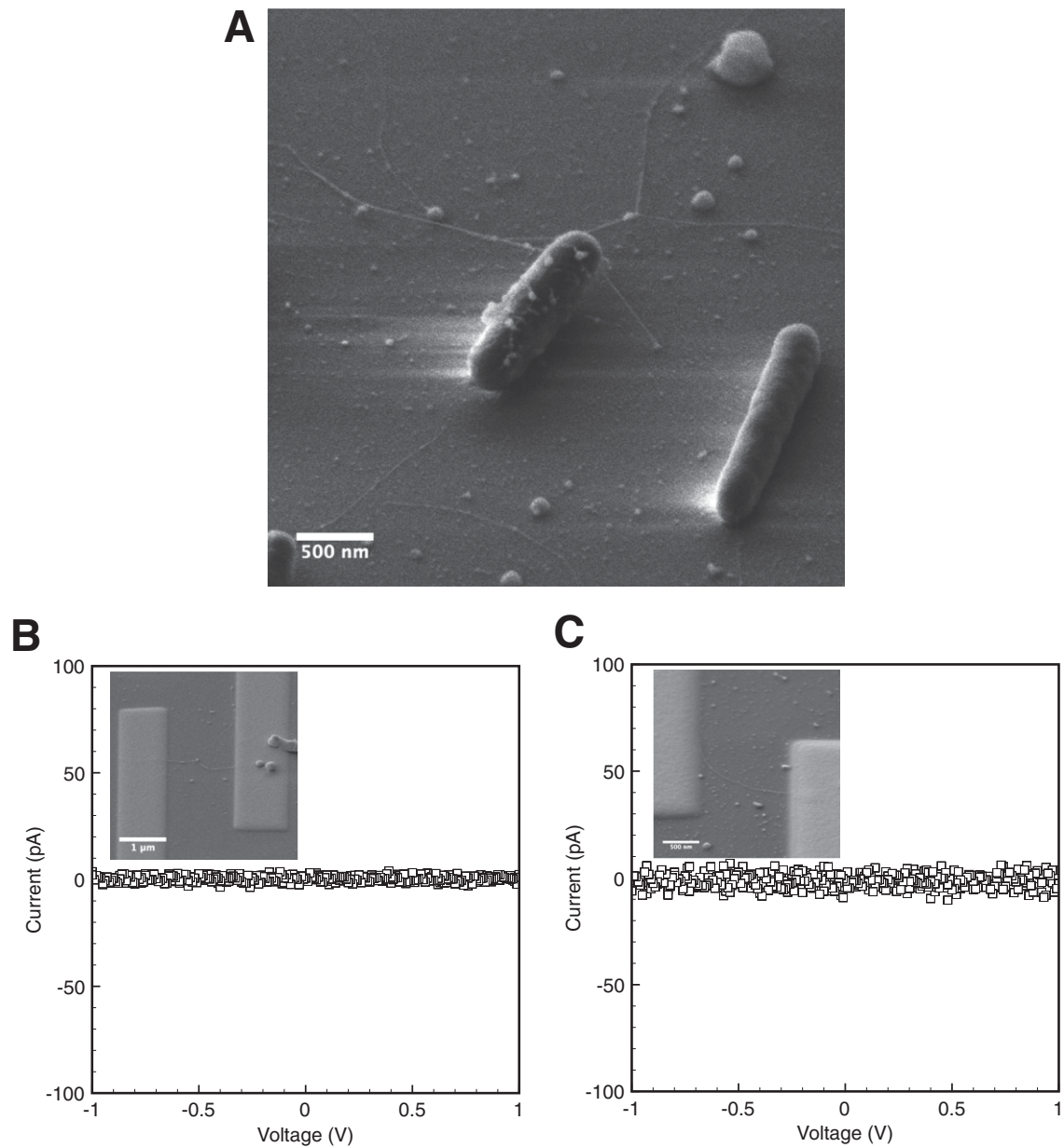


**Fig. S2.** Measurements of extracellular appendages from  $\Delta mtrC/omcA$  mutants. (A) SEM image of a  $\Delta mtrC/omcA$  mutant cell showing extracellular appendages morphologically consistent with bacterial nanowires. (B and C) I-V sweeps indicating two nonconductive appendages (SEM images in *Inset*) from  $\Delta mtrC/omcA$  mutant cells (a total of seven mutant wires were tested, all nonconductive).



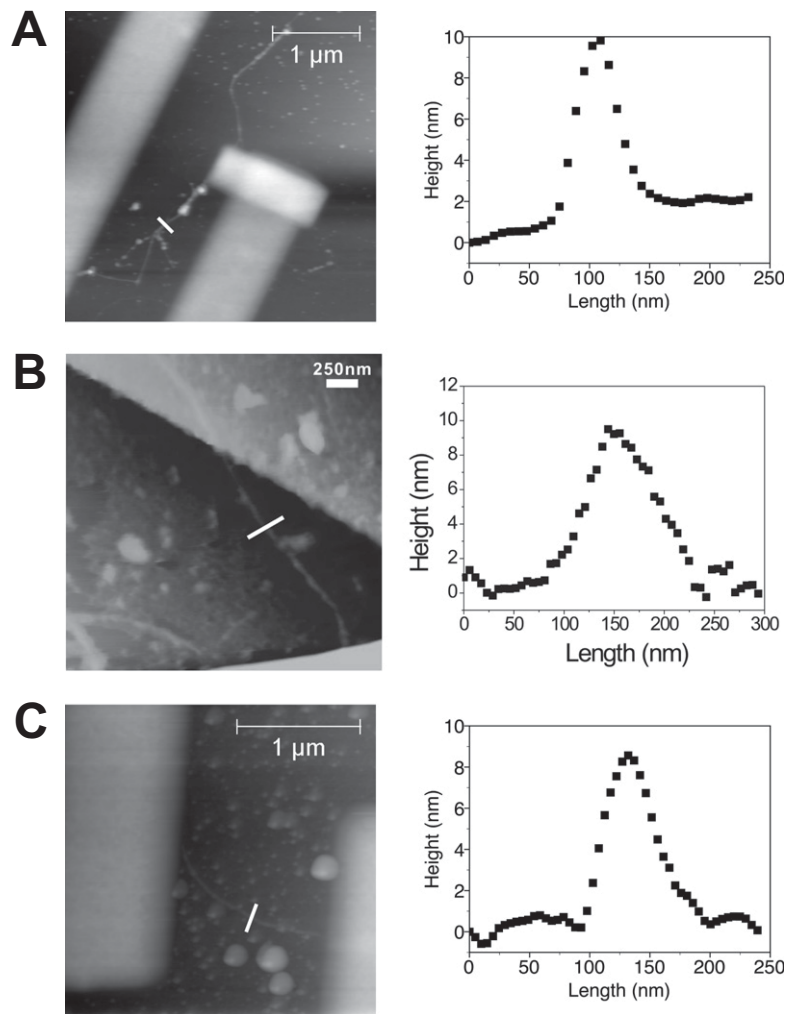


**Fig. 54.** AFM topography images and height profiles for the three types of samples analyzed in this study. (A) Bacterial nanowire from wild-type *S. oneidensis* MR-1 between two nanofabricated electrodes. (B) Bacterial nanowire from wild-type *S. oneidensis* MR-1 investigated using CP-AFM. (C) Nonconductive extracellular appendage from  $\Delta mtrC/omcA$  between nanofabricated electrodes.